Cardiac Activity Impacts Cortical Motor Excitability

Esra Al (esraal@cbs.mpg.de)
Max Planck Institute for Human Cognitive and Brain Sciences https://orcid.org/0000-0002-0582-4231
Tilman Stephani (stephani@cbs.mpg.de)
Max Planck Institute for Human Cognitive and Brain Sciences https://orcid.org/0000-0003-3323-3874
Melina Engelhardt (melina.engelhardt@charite.de)
Charité – Universitätsmedizin Berlin
Saskia Haegens (shaegens@gmail.com)
Columbia University
Arno Villringer (villringer@cbs.mpg.de)
Max Planck Institute for Human Cognitive and Brain Sciences
Vadim Nikulin (nikulin@cbs.mpg.de)
Max Planck Institute for Human Cognitive and Brain Sciences

Article

Keywords: cognition, somatosensory perception, cardiac cycle

DOI: https://doi.org/10.21203/rs.3.rs-1023617/v2

Additional Declarations: There is **NO** Competing Interest.

Cardiac Activity Impacts Cortical Motor Excitability

Esra Al[a,b,c,d,e*], Tilman Stephani[a,f], Melina Engelhardt[g,h], Saskia Haegens[d,e,i], Arno Villringer,[a,b,c], Vadim N. Nikulin[a,j]

a- Department of Neurology, Max Planck Institute for Human Cognitive and Brain Sciences, 04103 Leipzig, Germany

b- MindBrainBody Institute, Berlin School of Mind and Brain, Humboldt-Universität zu Berlin, 10099 Berlin, Germany

c- Center for Stroke Research Berlin (CSB), Charité – Universitätsmedizin Berlin, 10117 Berlin, Germany

d- Department of Psychiatry, Columbia University, New York, NY, USA

e- Division of Systems Neuroscience, New York State Psychiatric Institute, New York, NY, USA

f- International Max Planck Research School NeuroCom, 04103 Leipzig, Germany

g- Charité – Universitätsmedizin Berlin, Klinik für Neurochirurgie, 10117 Berlin, Germany

h- Charité – Universitätsmedizin Berlin, Einstein Center for Neurosciences, 10117 Berlin, Germany

i- Donders Institute for Brain, Cognition and Behaviour, Radboud University, Nijmegen, The Netherland

j- Institute of Cognitive Neuroscience, National Research University Higher School of Economics, 101000 Moscow, Russia

*Corresponding author. Email: esraal@cbs.mpg.de

Abstract

Human cognition and action can be influenced by internal bodily processes such as heartbeats. For instance, somatosensory perception is impaired both during the systolic phase of the cardiac cycle and when heartbeats evoke stronger cortical responses. Here, we test whether these cardiac effects originate from overall changes in cortical excitability. Cortical and corticospinal excitability were assessed using electroencephalographic and electromyographic responses to transcranial magnetic stimulation while concurrently monitoring cardiac activity with electrocardiography. Cortical and corticospinal excitability were found to be highest during systole and following stronger cortical responses to heartbeats. Furthermore, in a motor task, hand-muscle activity and the associated desynchronization of sensorimotor oscillations were stronger during systole. These results suggest that systolic cardiac signals have a facilitatory effect on motor excitability – in contrast to sensory attenuation that was previously reported for somatosensory perception. Thus, distinct time windows may exist across the cardiac cycle that either optimize perception or action.

Teaser

Heartbeats exert strong effect on motor activity by modulating cortical excitability.

Introduction

How we perceive and engage with the world is influenced by the dynamic relationship between the brain and the rest of the body including respiratory, digestive, and cardiac systems (*1*–*6*). For example, cardiac activity has been found to influence visual and auditory perception (*7*–*9*). In the domain of somatosensation and pain, perception and neural processing of stimuli have been reported to decrease during the systolic compared to the diastolic phase of the cardiac cycle (*10*–*13*). An overall systolic dampening of cortical processes was suggested to be due to baroreceptor activation during systole (*14*). In support of this view, reaction times to detect auditory, visual and tactile stimuli have been shown to be slower for systolic presentation (*15*, *16*). However, for some other motor movements, a facilitatory effect of systole has been observed, e.g., (micro)saccades occur more often during systole (*17*, *18*). (though these facilitatory effects might be due to blood movement in the body, rather than a top-down neural effect (*17*). Similarly, self-initiated movements have

been reported to occur more frequently during systole (*19*) or around the R-peak (*20*; but see (*21*). An effect of the cardiac cycle was also observed on gun shooting, with shooters preferentially triggering a gun in a cardiac window that included a large part of systole and initial part of diastole (*22*). In addition to cardiac phase effects, stronger neural responses to heartbeats, i.e., heartbeat-evoked potentials, are followed by increases in visual perception and decreases in somatosensory detection (*11*, *13*, *23*). It is therefore established that cardiac activity interacts with both perception and action. What remains unknown are the underlying mechanisms of these effects.

One possibility is that cardiac activity exerts its effects through alterations of neuronal excitability in different parts of the brain. A few previous studies have investigated this hypothesis using transcranial magnetic stimulation (TMS) over the primary motor cortex, which induces motor-evoked potentials, an indicator of corticospinal excitability. However, so far, no main effect of the cardiac phase on excitability levels has been observed (*24–27*). Otsuru et al. (*26*) showed corticospinal excitability 400 ms after R-peak to be significantly higher in poor compared to good interoceptive perceivers but the authors did not observe a significant main effect of cardiac phase on motor excitability. There are several possible methodological reasons for these findings. Importantly, the examination of excitability was limited to specific time intervals (only up to 400 ms after R-peak), rather than across the entire cardiac cycle including both systolic and diastolic window. Furthermore, individual brain anatomy was not taken into consideration, possibly resulting in higher variability of the stimulated brain regions. Lastly, these previous studies only included peripheral measures of corticospinal excitability without direct measurement of cortical excitability via concurrent electroencephalography (EEG) recordings.

In the present study, we systemically examine whether cortical and corticospinal excitability change across the entire cardiac cycle, and whether they interact with heartbeat-evoked potentials. Neuro-navigated TMS was used in combination with multichannel EEG, in order to comprehensively investigate both cortical and peripheral TMS-evoked responses. If systolic activity attenuates motor excitability, similar to somatosensory perception, TMS pulses during systole would be expected to produce weaker motor-evoked potentials in the hand muscle and weaker TMS-evoked potentials in the motor cortex. Similarly, increases in

heartbeat-evoked potentials would be expected to attenuate upcoming motor excitability. Alternatively, if behavioral observations of motor facilitation during systole are correct (*17*–*19*, *22*), stronger MEPs and TMS-evoked potentials should be observed. Supporting this latter hypothesis, we found that both peripheral and central TMS-evoked potentials were in fact higher during systole. Moreover, stronger heartbeat-evoked potentials preceded increases in excitability. In line with these findings, hand-muscle activity and associated desynchronization of sensorimotor oscillations in a motor pinch task were strongest during the systolic heart phase. Taken together, our results reveal that there is a faciliatory effect of systolic activity on motor excitability, possibly connected with an optimal window for action initiation during the cardiac cycle.

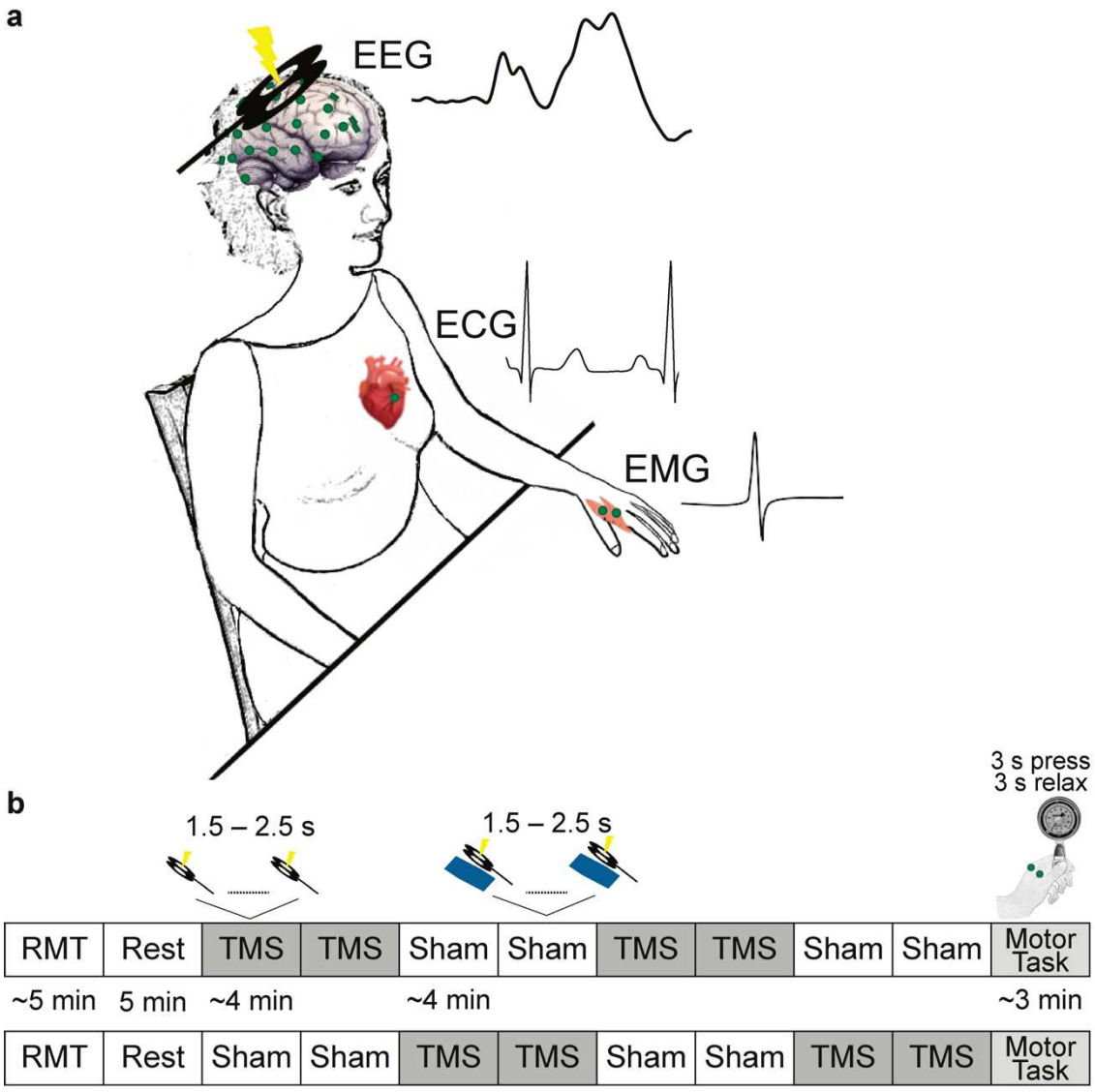

Figure 1. Experimental Paradigm. (**a**) TMS was applied over the right primary motor cortex of the subjects. The motor response to TMS in their left hand, i.e., motor-evoked potential (MEP), was measured by bipolar electromyography (EMG). Their cortical responses to TMS, the TMS-evoked potential (TEP), as well as to heartbeats, the heartbeat-evoked potential (HEP), were measured using multichannel electroencephalography (EEG). The heart activity was recorded via electrocardiography (ECG). (**b**) After determining the individual resting motor threshold (RMT), subjects underwent a resting-state EEG measurement. Thereafter, 416 single TMS pulses with an intensity of 120% of the RMT were applied in four blocks. There were also four blocks of sham conditions, in which a plastic block was placed between the TMS coil and the head of the subject. The pairs of real and sham TMS blocks were randomized across the subjects. At the end of the TMS blocks, participants performed a motor pinch task. In this task, they were instructed to squeeze a pinch gauge with their left thumb against the index finger while a red circle was presented in the middle of the monitor. When the circle became green, they relaxed their fingers. In this order, subjects performed thirty trials.

Results

Motor-evoked potentials change across the cardiac cycle

To test whether the cardiac phase influences corticospinal excitability, we stimulated the right primary motor area with TMS across the cardiac cycle and recorded motor-evoked potentials (MEPs) of the first dorsal interosseus muscle in the left hand in thirty-six participants (**Fig. 1**). Consistent with the notion of corticospinal excitability changes across the cardiac cycle, MEP amplitudes were significantly higher during systole to diastole (*Wilcoxon signed rank test, V=463*, $p = 0.040$, Cohen's $d = 0.341$; **Fig 2**). As an additional control of a potential effect of ECG artefact on EMG activity, systolic and diastolic EMG activity during the sham condition was subtracted from real TMS activity. After this control analysis, MEP amplitudes remained significantly higher during systole (*V=463*, $p = 0.041$, Cohen's $d = 0.340$).

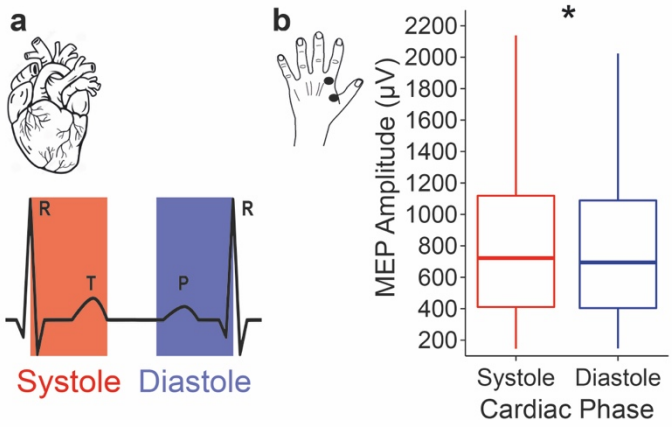

Figure 2. Changes in corticospinal excitability depending on the timing of TMS application across the cardiac cycle. (**a**) Schematic of the cardiac cycle. The systolic phase (indicated in red) starts with the R-peak and reflects the ventricular contraction of the heart (leading to blood ejection), whereas the diastolic phase (indicated in blue) represents the relaxation phase during which the heart refills with blood. (**b**) MEP amplitudes of the first dorsal interosseus muscle in the left hand are higher in response to TMS stimulation during systole (red) compared to diastole (blue). *$p < 0.05$

TMS-evoked potentials vary across the cardiac cycle

In addition to corticospinal excitability, we also systematically tested the changes of cortical excitability between the systole and diastole phases of the cardiac cycle using EEG. Cortical excitability was probed by early TMS-evoked potentials (TEPs; 15 - 60 ms post-TMS) measured from a cluster of electrodes (C4, CP4, C6, CP6) over the right motor cortex (hotspot). TEP amplitudes between 22 to 60 ms following the TMS stimulation were stronger during systole as compared to diastole (cluster-based permutation *t*-test, $p_{cluster} = 0.009$; Cohen's d = 0.41, **Fig. 3a**). To test whether these results were indeed related to neural activity of the cortex, rather than reflecting TMS- and cardiac-artifacts, we contrasted them with stimulus-locked EEG signals of the sham TMS condition. A cluster-based permutation test did not reveal any significant difference in TEPs in response to sham TMS during systole and diastole ($p_{cluster} = 0.2$, **Fig. 3b**). Furthermore, to account for physiological and stimulation artifacts, TEPs during sham were subtracted from those in the real TMS condition. The TEP difference was significantly higher between 24 and 60 ms during systole relative to diastole ($p_{cluster} = 0.008$, Cohen's d = 0.41, **Fig. 3c**). The corresponding neural sources of the TEP difference between systole and diastole were observed to be maximal around the right primary motor cortex (**Fig. 3d**).

We next analyzed whether the phasic modulation of MEP amplitudes and TEPs (over motor electrodes in the significant cluster window of 24-60ms) across the cardiac cycle are related. This initial analysis showed no significant correlation between the MEP and TEP differences between systole and diastole (Pearson's r= 0.26, p=0.121). In a further exploratory analysis, we tested whether the cardiac changes in MEP amplitudes correlate with the modulation of earlier TEP activity since the changes in MEP amplitudes have been shown to correlate significantly with P30 or N15-P30 peak-to-peak amplitudes (*28*), but not P60 component of

TEP(*29*). This analysis revealed a significant positive correlation between the cardiac modulation of MEP and TEPs, r=0.35, p=0.038.

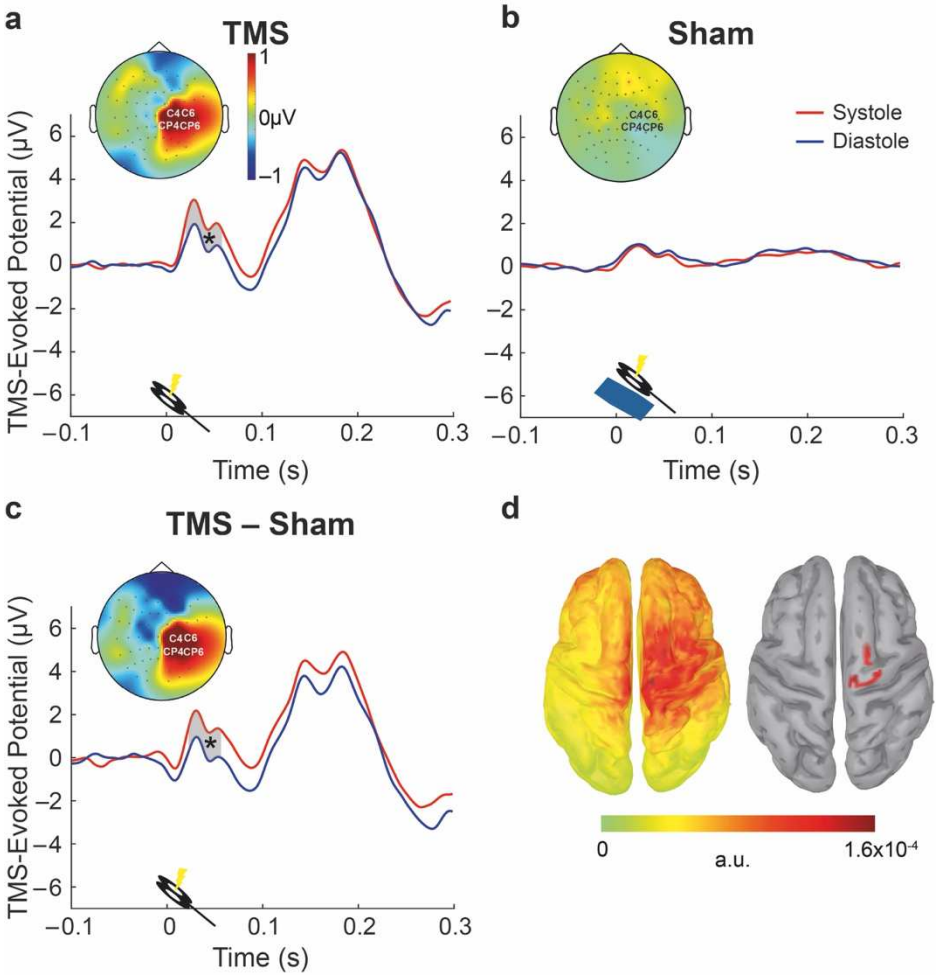

Figure 3. Changes in cortical excitability across the cardiac cycle. (**a**) TMS-evoked potentials (TEPs), in response to TMS stimulation, at the electrodes closest to the motor hotspot (C4; CP4; C6; CP6). Early TEPs were significantly larger during systole compared to diastole in motor areas between 22 and 60 ms. The contrast between systole and diastole in this time window is shown in the topography plot. (**b**) Same as in a, for the sham TMS condition. No significant differences between systole and diastole were observed here. (**c**) The difference curve between real TMS and sham, for systole and diastole (sham-corrected TEP contrast). After correcting for the TMS and physiological artifacts, TEPs during systole and diastole were significantly different between 24 and 60 ms. (**d**) The source reconstruction of the corrected TEP contrast (systole minus diastole) between 24 and 60 ms (left), and same displaying the strongest generators only (thresholded at 85% of the maximum activity and clusters sizes of at least five vertices; right).

Muscle-related peripheral and central activity fluctuates across the cardiac cycle

In a follow-up motor pinch task, we then investigated whether higher motor excitability during systole was associated with an increase in the actual muscle activity during systole. For

this purpose, we recorded EMG, EEG, and ECG activity while subjects were performing a motor pinch task, where they were asked to pinch a dynamometer with their index finger and thumb (**Fig. 4a**). To estimate peripheral muscle force, we calculated the linear envelope of EMG activity when subjects initiated the pinch during systole and diastole. Cluster statistics revealed a significant increase in the normalized EMG envelope from 220 to 522 ms after the onset of the pinch, during systole compared to diastole ($p_{cluster} = 0.011$, Cohen's $d = 0.46$, **Fig. 4a**). To test whether this finding might have been related to blood circulation-related changes in the fingers, we sampled systolic and diastolic EMG activity during the resting state condition. This analysis did not reveal any significant difference in the resting EMG envelope between systole and diastole (no significant clusters were found). This indicates that there was no influence of cardiac-related artifacts on the EMG signal across the cardiac cycle.

Following the analysis of the muscle activity in the periphery, we also tested whether sensorimotor oscillations (in the range of $8-30$ Hz) in the motor areas desynchronize differently following the initiation of the pinch during systole and diastole. This analysis demonstrated that the desynchronization of sensorimotor oscillations in the range of $8-25$ Hz was stronger between 0 and 726 ms following pinch onset during systole as compared to diastole ($p_{cluster} = 0.012$, Cohen's $d = 0.37$, **Fig. 4b, c**). To investigate whether this finding was influenced by cardiac-related artifacts, we again sampled systolic and diastolic windows during the resting state and tested the differences in sensorimotor oscillations between systole and diastole. Also, in this control analysis, no significant differences were found ($p_{cluster} = 0.12$). Thus, these results indicate that both peripheral muscle activity and its central correlates are stronger when the movement starts during systole as compared to diastole.

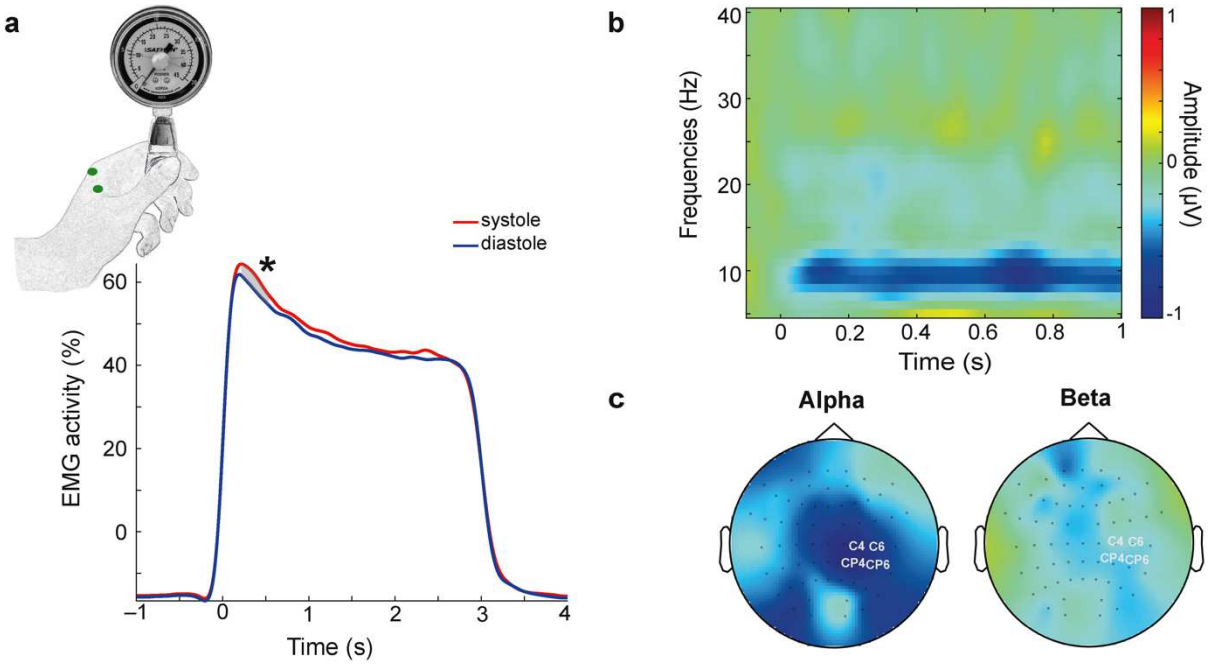

Figure 4. Fluctuations of muscle-related activity depending on the pinch onset across the cardiac cycle during a motor pinch task. (**a**) Muscle force, measured by the normalized linear envelope of EMG activity, in the left hand, was significantly higher from 220 to 522 ms following pinch onset (at 0 ms) during systole compared to diastole. (**b**) Similarly, systolic and diastolic sensorimotor oscillations were analyzed in the range of 8 – 30 Hz in the sensorimotor electrodes to quantify event-related desynchronization following the muscle activation. Cluster statistics revealed that when subjects started the pinch during systole, the desynchronization of sensorimotor oscillations was higher in the frequency range of 8 – 25 Hz between 0 and 726 ms following pinch onset. The raster plot shows the contrast between systole and diastole. (**c**) The topography of this significant contrast is also shown individually for alpha (8 – 13 Hz) and beta (14 – 25 Hz) sensorimotor oscillations.

Heart rate changes depending on the timing of TMS across the cardiac cycle

We further investigated the changes in the heart rate in response to TMS stimulation during systole and diastole across time (pre-TMS, TMS, post-TMS). The analysis showed a main effect of time ($F_{2, 70} = 23.11$, $p = 2 \cdot 10^{-8}$) and an interaction of time and cardiac phase ($F_{2, 70} = 10.30$, $p = 1 \cdot 10^{-4}$) on heart rate. Comparison of heartbeat intervals preceding TMS and concurrent with TMS revealed a significant cardiac deceleration when TMS stimulation occurred during systole ($t_{35} = -5.73$, $p = 2 \cdot 10^{-6}$, Cohen's d = 0.96). This was followed by a cardiac acceleration (from TMS to post-TMS; $t_{35} = 8.58$, $p = 4 \cdot 10^{-10}$, Cohen's d = 1.43, **Fig. 5**). No significant changes were observed for stimulations during diastole (from pre-TMS to TMS, $t_{35} = 0.75$, $p = 0.5$ and from TMS to post-TMS, $t_{35} = 0.42$, $p = 0.68$, **Fig. 5**). Post-hoc *t*-tests showed that there was no

significant difference in heart rate before TMS stimulation between systole and diastole ($t_{35} = 1.83$, $p = 0.075$), whereas the heart rate difference was significant during TMS stimulation ($t_{35} = 2.10$, $p = 0.043$, Cohen's d = 0.35). This difference was no longer statistically significant in the post-TMS window ($t_{35} = 1.80$, $p = 0.080$).

To control whether these heart rate changes were due to genuine effects of TMS rather than artifacts (e.g. auditory, somatosensory) induced by TMS application, heart rate across time was adjusted with the heart rate during the sham TMS condition individually for each time interval and cardiac phase. This analysis again showed a similar main effect of time ($F_{2, 70} = 7.42$, $p = 1 \cdot 10^{-3}$) and an interaction of time and cardiac phase ($F_{1.56, 54.64} = 3.88$, $p = 0.03$) on heart rate.

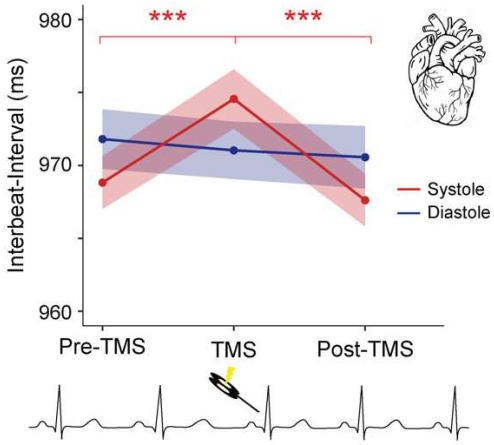

Figure 5. Heart rate changes induced by TMS are influenced by the cardiac cycle. The heart first slowed down and then accelerated when TMS pulses were delivered during systole. No significant differences were observed for stimulations during diastole. Colored bands indicate 95% within-participant confidence intervals(*66*). ***$p < 0.0005$

Heartbeat-evoked potentials fluctuate depending on motor excitability levels

In addition to the cardiac phase effects, we examined the relationship between motor excitability and preceding cortical responses to heartbeats, so-called heartbeat-evoked potentials (HEP). To be able to distinguish cardiac and TMS-related neural processing, we first only chose trials in which the TMS stimulation occured at least 400 ms after the preceding R-peak in line with the previous studies (*11*, *13*). This allowed us to investigate the relationship of HEPs (during systole) with MEPs (during diastole) within the same cardiac cycle. For this purpose, we sorted single trials according to their MEP amplitudes and split them into three equal bins for each participant. The sorting was done according to MEP amplitudes since they are observed in every single trial included in the analysis. We then contrasted prestimulus

HEP amplitudes preceding weak and strong MEP levels by using a cluster-based permutation *t*-test in the *296 – 400* ms *post R-peak time window* in the centroparietal electrodes as identified in previous studies (*11*, *13*). HEPs were significantly higher preceding strong compared to weak MEP amplitudes, between 304 and 324 ms over the centroparietal electrodes ($p_{cluster}$ = 0.021 corrected for multiple comparisons in space and time; Cohen's d = 0.48, **Fig. 6a, b**). We then asked whether MEP amplitudes during the first 400 ms of the cardiac cycle are influenced by HEP activity in response to the previous cardiac cycle. This analysis showed that HEP amplitudes were more positive between 362 and 394 ms at centroparietal electrodes preceding strong compared to weak MEP amplitudes ($p_{cluster}$ = 0.018 corrected for multiple comparisons in space and time; Cohen's d = 0.53; **Supplementary Fig. 1**).

To test whether these effects are induced by overall changes in cardiac activity during TMS stimulation, we further tested the differences in HEP activity during TMS stimulation and resting-state condition (without TMS stimulation). No significant differences in HEP amplitudes during TMS and resting-state were observed (no clusters were found; **Supplementary Fig. 2**).

Heart rate fluctuates depending on motor excitability levels

We furthermore investigated the effect of motor excitability on heart rates. For this purpose, we tested the relationship between interbeat-intervals, that is, the duration between two consecutive heartbeats, and MEP amplitudes. Increases in MEP amplitudes correlated with decreases of the interbeat-intervals (repeated measures correlation, r = - 0.48, $p = 2 \cdot 10^{-5}$, **Fig. 6c**). In other words, as motor excitability increased, the heartbeats became faster (cardiac acceleration). As a control analysis, we also tested whether heart rates differed between the resting-state condition and during TMS application. No significant differences in heart rate were observed here (t_{35} = 0.28, p = 0.78).

We furthermore tested whether there is a relationship between the changes in heart rate due to the cardiac timing of TMS and excitability levels. The changes in heart rate as a result of systolic as compared to diastolic stimulation did not significantly correlate with heart rate changes between high and low corticospinal excitability levels (Spearman's rank correlation,

$r = -0.16$, $p = 0.36$). Therefore, cardiac timing of TMS and excitability levels seem to have different effects on heart rate, which in turn suggests that cardiac phase effects on excitability are not likely to be explained by changes in heart rate.

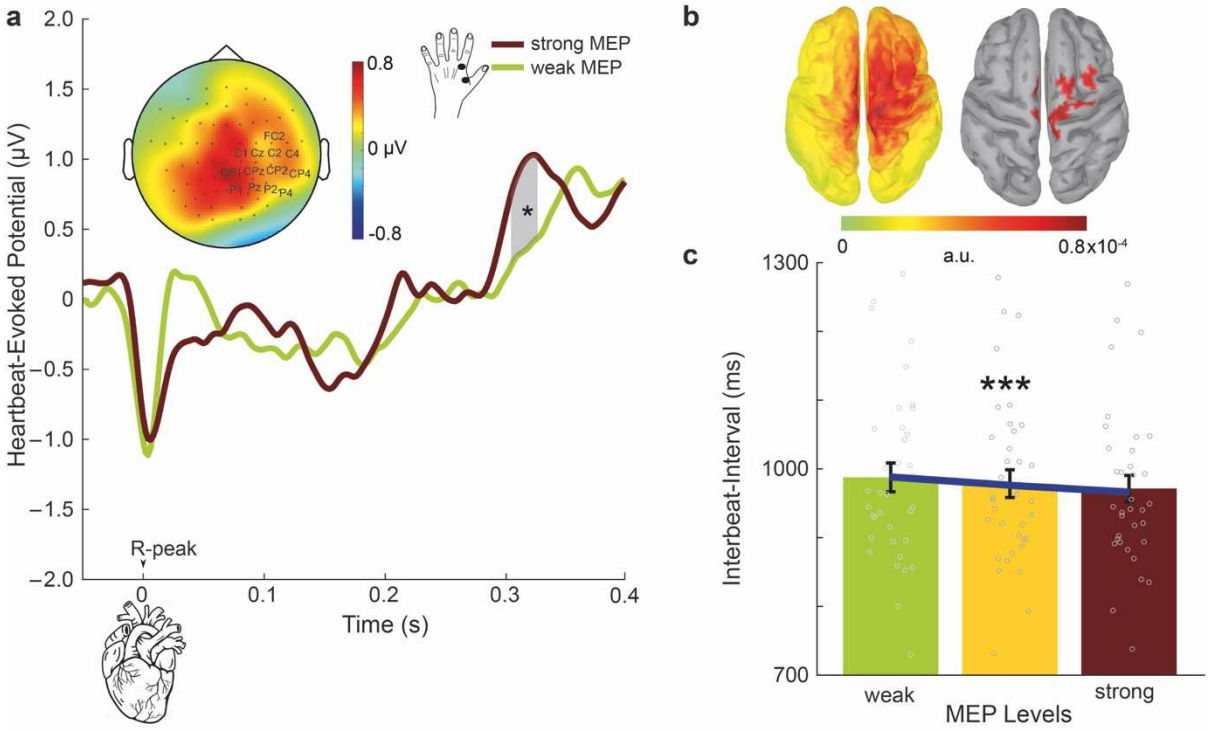

Figure 6. The cortical responses to heartbeats, heartbeat-evoked potentials (HEPs), preceding changes in the strength of motor excitability. (**a**) To assess relationship between HEPs and motor excitability, single trials were sorted according to MEP amplitudes and split into three equal bins for each subject. HEP amplitudes between 304 and 328 ms following the R-peak (the highlighted gray area) were higher preceding strong compared to weak motor-evoked potentials (MEPs) across the centroparietal electrodes. The topography contrast represents HEP amplitude difference preceding strong versus weak MEPs between 304 and 328 ms. (**b**) (left) The neural sources of HEP differences preceding strong and weak MEPs are visualized. (right) Same as the left figure but displaying the strongest generators only (thresholded at 85% of the maximum activity and clusters sizes of at least five vertices). (**c**) Interbeat-interval became shorter for stronger MEP amplitudes. In other words, subjects' motor excitability increased as their heart beat faster. *$p<0.05$, ***$p<0.0005$.

Control analyses for movement of cortex across the cardiac cycle

Next, we investigated whether our findings of larger motor excitability during systole might have been related to the displacement of the cortex due to blood influx and efflux (as a result of cardiac activity). The mechanical displacement of the cortex follows an inverse u-shaped

pattern across the cardiac cycle, rather than a linear relationship, and it reaches its maximum at 450-500 ms after the R-peak(*30*). To observe whether MEP amplitudes followed a similar pattern across the cardiac cycle, we first visualized MEP amplitudes across 50ms bins following the previous R-peak (**Supplementary Fig. 3**). This demonstrated that MEPs were maximal during the first 50 ms and gradually decreased across the cardiac cycle. To statistically test the relationship between MEP amplitudes and the distance from the previous heartbeat, linear-mixed-effects model regressions were fit on the single-trial level. The linear regression that included the cardiac distance (MEP ~ distance + (1 | subject)) explained the empirical data better than the null model, i.e., a model with no relationship assumed (MEP ~ (1 | subject); $\chi^2 = 4.67$, $p = 0.03$). Crucially, this linear model also showed a better fit than a second-degree polynomial model (MEP ~ distance + distance^2+ (1 | subject), $\chi^2 = 0.34$, $p = 0.6$). This result indicates that the changes in MEP amplitudes do not follow a u-shaped pattern across the cardiac cycle and are thus not likely to be explained by the displacement of the cortex due to blood influx or efflux.

Discussion

Using simultaneous recordings of cortical, cardiac, and muscle activity with EEG, ECG, and EMG in response to TMS stimulation, we found that cardiac signals and their neural processing were associated with changes of motor excitability. More specifically, corticospinal excitability, probed by motor-evoked potentials in the FDI muscle of the left hand, was significantly higher when TMS coincided with the systolic as compared to the diastolic phase of the cardiac cycle. In line with changes in corticospinal excitability, we further showed that cortical excitability, as measured by TMS-evoked potentials in the motor cortex, was stronger during systole. Moreover, consistent with this finding, in the motor pinch task we observed that muscle activity and desynchronization of sensorimotor oscillations were stronger following muscle contractions during systole (as compared to diastole). Furthermore, we observed significant modulations of heart rate when TMS was presented during systole, while diastolic stimulations did not trigger any significant changes in heart rate. In addition to cardiac timing effects, increases in cortical responses to heartbeats, as measured by heartbeat-evoked potentials, predicted stronger corticospinal excitability, which also correlated positively with heart rate. These results are unlikely to reflect

stimulation artifacts since both heartbeat-evoked potentials and heart rates were comparable between resting-state and TMS conditions.

Methodological differences are likely to explain the absence of cardiac modulation of motor excitability in previous TMS studies(*24–26*). In those studies, time resolution across the cardiac cycle was rather limited. Unlike in our study, TMS stimulations were not presented throughout the entire cardiac cycle, they were rather presented up to 400 or 600 ms after the heartbeats and at specific time points (e.g., 100 ms after R-peak). Since our study revealed a linear decrease in motor excitability throughout the cardiac cycle, previous studies might not have been able to sample the decrease towards the end of the cardiac cycle. Furthermore, combining a neuro-navigational system with individual brain scans provided us with a higher spatial specificity for the stimulation location, in comparison to previous studies. In addition, our study had the advantage of a larger sample size and trial numbers, which contributed to higher statistical power to detect the cardiac-cycle effects on motor excitability (*24–26*). Since the observed MEP effect was rather small in our study, a larger set of participants (as in the present study) would indeed facilitate a statistical detection of differences. Finally, previous studies only tested cardiac effects on peripheral MEPs without concurrent cortical recordings. Yet, it is known that peripheral MEPs reflect excitability changes at both cortical and spinal-cord levels and special measures should be taken (such as H-reflex) in order to disentangle excitability changes between these two levels (*31*). On the other hand, TEPs directly reflect changes in cortical excitability, especially at early latencies (*32*). This can also explain why we observed a stronger effect size for the cardiac modulation of TEPs as compared to MEPs.

Cardiac cycle effects on motor excitability are consistent with previous findings of increased frequency of muscle movement during systole as compared to diastole (*17–19*, *22*). Here, we showed that TMS during systole is associated with higher corticospinal and cortical excitability in motor areas. Thus, motor-related activity seems to be facilitated during systole. This in turn may also explain why eye movements (*17*, *18*), e.g., (micro)saccades, and voluntary hand movements (*22*), e.g., firing a gun, have been found to occur more often during systole. One could also argue that the effects we found were merely due to the fact that the distance of the brain to the skull (and thus the TMS coil) changes due to fluctuations in intracranial pressure throughout the cardiac cycle (*33*). This, in turn, should affect the induced electric

field from TMS. However, our control analyses did not support this argument. More specifically, the movement of the brain follows an inverse u-shaped pattern across the cardiac cycle and reaches a maximal distance at about 450-500 ms after the previous heartbeat(*30*). If the cortical movement across the cardiac cycle was responsible for the cardiac phase effects, then MEPs would be expected to follow a similar pattern across the cardiac cycle. However, MEP amplitudes decreased rather linearly across the cardiac cycle, differently than effects that would be expected due to cortical movement. This result indicates that the changes in MEP amplitudes are not likely to be explained by the displacement of the cortex across the cardiac cycle. Another possible artifact, which can influence the amplitude of the evoked activity, are muscle-related far-fields from the cardiac activity (typically referred to as "cardiac artifacts" in the EEG). To control for those, we included a sham condition, in which auditory, tactile, and cardiac artifacts were comparable. After the correction of real TMS recordings with the sham condition, cortical excitability was still significantly higher during systole as compared to diastole. Overall, these results suggest that motor excitability is higher during systole, suggesting an optimal window for motor activity across the cardiac cycle.

The cardiac cycle was also observed to affect muscle activity in a motor task, where subjects were asked to pinch and release a dynamometer with their left index finger and thumb. When the pinch was initiated during systole, compared to diastole, muscle activity was transiently stronger, suggesting a systolic increase in the applied force (*34*). In addition to the peripheral activity, we analyzed cardiac effects on the central neural activity during the motor task. Previous studies have shown that following muscle contractions, sensorimotor oscillations desynchronize in the motor regions, which is reflected as an amplitude decrease in the alpha and beta range (*35*, *36*). Here, we found that this desynchronization transiently increased when the pinch was initiated during systole. Furthermore, these cardiac effects on the muscle-related activity are not likely due to cardiac artifacts, since no significant differences in muscle and neural activity were observed across the cardiac cycle while subjects were resting. Overall, these findings suggest that muscle activity is stronger when movement is initiated during systole due to an increase in motor excitability.

The increased motor excitability during systole seems to be at odds with the previously shown cardiac effects on perception. For example, we recently demonstrated that somatosensory

percepts and their neural processing are attenuated during systole (*11*, *13*). We explained these findings by an interoceptive predictive coding account, which postulates that rhythmic cardiac signals are predicted and suppressed from entering conscious perception. This mechanism was suggested to additionally inhibit the perception of coincident weak external stimuli (*11*, *13*). Furthermore, this suppression of non-salient sensory stimuli was suggested to lead to a greater uncertainty about threatening factors in the environment (*37*). To compensate for it, the organism might increase expectation for a "risk" and use its limited resources for a "flight or fight" motor response, which can be potentially mediated by increased baroreceptor activity during systole. Therefore, it is possible that the increased motor activity during systole might provide a survival advantage. Hence, this would suggest that there are different optimal windows for action and perception throughout the cardiac cycle. This idea also fits well with previous studies on "sensory gating", in which somatosensory perception and evoked potentials were shown to be attenuated during movement(*38–40*). Given that action has an inhibitory effect on perception, it is plausible that systolic facilitation of action is indeed consistent with inhibition of perception during the systolic phase of the cardiac cycle.

It is also important to note that different cardiac effects occur within the systolic and diastolic cardiac phases. During systole, in response to changes in blood pressure, baroreceptors become maximally active approximately 300 ms after R-peak (*41*). This change in baroreceptor activity has been suggested to be the driving force of the cardiac effects on perception. For example, during this time window, the processing of somatosensory and pain stimuli is maximally affected (*11*, *13*, *42*). However, in the current study, we observed that motor excitability was strongest during the pre-ejection period of the systole, before arterial pressure starts to increase and activate baroreceptors. Therefore, the cardiac-related effects on the motor domain might not be mediated by baroreceptor activity, but via a direct neural pathway involving cardiac afferent neurons that fire around the R-wave and have a fast conduction velocity leading to a rapid cortical activation (*43*). Future studies could investigate this idea by using animal models.

Cortical excitability changes have been associated previously with epilepsy, chronic insomnia, disorders of consciousness, stroke, and depression. To counterbalance these abnormalities in

cortical excitability, the therapeutic applications of TMS have been introduced, e.g., for treating depression (*44*) or facilitating recovery during neurorehabilitation (*45*). Our results on cardiac modulations of cortical excitability raise some important questions for these clinical populations. For example, it remains unknown whether cortical excitability over the cardiac cycle is modulated in those pathological conditions. Furthermore, our observation that TMS induces changes of the heart rate during systole, i.e., when the cortical processing of heartbeats occurs, but not during diastole, can have important implications for clinical use of TMS. When the changes in heart rate of patients during TMS application are a clinical concern, then our results indicate that stimulation during diastole can prevent these unwanted changes. In contrast, synchronization of TMS with systolic activity might be relevant for treatment of clinical subgroups, such as depression, which is often associated with decreased heart rate variability and increased heart rate (*46–48*). Our results, therefore, suggest that application of TMS during systole or diastole might be helpful to optimize clinical protocols, which should be addressed in future studies.

Another effect of cardiac activity on motor excitability was found on the cortical level. We observed that heartbeat-evoked potentials (HEPs), during systole, showed higher positivity over centroparietal electrodes between 304 and 328 ms preceding strong as compared to weak corticospinal excitability (as measured by TMS-induced MEPs). These results again diverge from our previous results on somatosensory perception, in which we observed higher HEPs preceding attenuated somatosensory processing. We previously explained increases in HEPs as a result of an attentional switch from the external world to internal bodily signals, such as heartbeats (*11*). This was further supported by higher HEP amplitudes when subjects were resting compared to engaging in an external task (*13*). If internal attention levels changed in the current study during the TMS condition compared to rest, we would expect lower HEPs during the TMS condition. However, in the current study, there was no significant change in HEPs during the TMS application in comparison to the resting state of the subjects. This was probably related to the absence of an external task during the TMS condition. Another factor, which can positively influence HEP amplitude, is arousal (*49*). Increases in arousal are also known to increase motor excitability (*50*) as well as heart rate (*1*, *51*). Supporting a possible involvement of arousal in our study, we observed that heart rate became higher as motor excitability increased. Therefore, we suggest that increases in

arousal might be responsible for increases in HEP amplitudes for stronger motor excitability. It is also possible that since this analysis involves HEPs and MEPs, which were close in time, there was a similar cortical state for both responses due to intrinsic neuronal dynamics. If the magnitude of both HEPs and MEPs reflects increased cortical excitability, then a positive correlation would be expected, since cortical excitability changes on many time scales (*52*), including a period covering both pre- and immediate post-stimulus intervals.

In conclusion, our study provides novel insights into the regulation of cortical and corticospinal excitability by cardiac function in healthy individuals. Together, these findings strongly suggest that systolic cardiac activity and its cortical processing have faciliatory effects on motor excitability, in contrast to the previous findings on somatosensory perception. Thus, we propose that optimal windows for action and perception may differ across the cardiac cycle. Furthermore, these results may contribute to the development of novel stimulation protocols and promote a better understanding of the interplay between brain dynamics and bodily states in both health and disease.

Methods

Participants

Based on our previous study in which we originally observed an effect of cardiac cycle on somatosensory perception (*12*), we did a power analysis (using the "pwr" package in R). Given a Cohen's d of 0.48, we calculated the required sample size as N=36 (80% power and alpha=0.05) for observing cardiac effects on perception.

For the experiment, we only invited subjects who were between 18 and 40 years old and who did not report any neurological, cognitive, or cardiac health problems. Exclusion criteria further included tinnitus, alcohol or drug abuse, and pregnancy. 37 healthy volunteers participated in the experiments after giving written informed consent. All protocols were approved by the Ethical Committee of the University of Leipzig's Medical Faculty (Ethics no: 179/19). One subject was excluded due to failure in the data acquisition. In the remaining 36 subjects (20 female, age: 27.97 ± 4.13, mean ± SD), only one subject was left- handed as assessed using the Edinburgh Handedness Inventory (*53*).

TMS setup and neuronavigation

The experiment included 4 blocks of sham and 4 blocks of real TMS stimulations. Participants were seated in a comfortable armchair and asked to keep their eyes on a fixation point on a wall in front of them throughout the measurements. TMS pulses were delivered through a Magstim 200 Bistim stimulator (Magstim Company Ltd, Whitland, UK) connected to a figure-of-eight coil (Magstim "D70 Alpha Coil"). The coil was positioned at an angle of 45° with respect to the sagittal direction. Structural T1 weighted MRIs of the subjects were used with the TMS neuronavigation system (Localite GmbH, Bonn, Germany) to identify the hotspot of the left first dorsal interosseous muscle (FDI). Then, the resting motor threshold was determined as the lowest TMS intensity at which 5 out of 10 trials yielded a motor response greater than 50 μV (peak-to-peak amplitude). The TMS blocks consisted of 104 trials, i.e., a total of 104 x 8 = 832 stimulations. The neuronavigation system was used to control the coil position over the hotspot during the TMS stimulations. TMS intensity was set to be 20% above the motor threshold at rest (corresponding to 66.58 ± 9.16% of the maximum stimulator output). The interstimulus interval was uniformly randomized between 1.5 and 2.5 seconds. The blocks were presented as pairs of two sham or real TMS and their order were randomized across participants. For the sham TMS condition, we used a custom-manufactured 3.5 cm plastic block between the coil and the participant's head to keep air- and bone-conducted auditory sensations similar to the real TMS (*54*). This setup also mimicked a tapping somatosensory sensation associated with the vibration of the TMS coil.

EEG, ECG and EMG recordings

TMS-compatible EEG equipment (NeurOne Tesla, Bittium) was used for recording EEG activity from the scalp. The EEG was acquired with a bandwidth of 0.16-1250 Hz from 62 TMS-compatible c-shaped Ag/AgCl electrodes (EasyCap GmbH, Herrsching, Germany) mounted on an elastic cap and positioned according to the 10–10 International System. POz electrode was used as ground. During the measurements, the EEG signal was referenced to an electrode placed on the left mastoid. Additionally, a right-mastoid electrode was recorded so that EEG data could be re-referenced to the average of both mastoid electrodes offline. The signal was digitized at a sampling rate of 5 kHz. Skin/electrode impedance was maintained below 5 kΩ. EEG electrode positions were also coregistered with the structural MRIs using the neuronavigation system. To reduce auditory response artifacts in the EEG induced by coil

clicks, participants wore earplugs throughout the experiment. An additional ECG electrode connected to the EEG system was placed under the participant's left breast to record the heart activity. Furthermore, EMG electrodes were attached to the left first dorsal interosseus (FDI) muscle in belly-tendon montage via a bipolar channel connected to the EEG system to record the TMS-induced motor-evoked potentials (MEP). At the beginning of the experiment, EEG and ECG data were acquired during a 5-min eyes-open resting-state measurement.

Automated Cardiac Phase Classification

The fluctuations of motor excitability were tested across the systolic and diastolic phases of the cardiac activity. Systole was defined as the time between the R-peak and the end of the t-wave, which was determined by using a trapezoid area algorithm (*11*, *55*). We then used the duration of systole to define an equal length of diastole at the end of each cardiac cycle (*11*). By using time windows of equal length for systole and diastole, we equated the probability of a stimulation/event occurring in either of the two phases. As a result, the average systole (and diastole) length was 351± 21 ms. Before using this automated algorithm, we removed large TMS artifacts on the ECG data by removing -2 to 10 ms window around the TMS stimulation and then applied cubic interpolation. As a result, the number of trials was not significantly different ($t35=-1.05$, $p=0.3$) between systolic (148±17) and diastolic (150±18) parts of cardiac cycle. Therefore, with this approach, we could ensure comparable trial numbers across conditions.

Motor-Evoked Potentials

As an index of corticospinal excitability, motor-evoked potentials (MEPs) were used. After applying a baseline correction using -110 to -10ms prestimulus window, peak-to-peak MEP amplitudes were calculated in the EMG data in the time window of 20 – 40 ms following the TMS stimulation. To investigate possible changes of MEP amplitude across the cardiac cycle, we contrasted the averaged MEP amplitudes between systole and diastole.

TMS-Evoked EEG Potentials

EEG data was first segmented between -1400 and 1000 ms around TMS stimulations. Then, the baseline correction was performed using -110 to -10ms prestimulus window. The large amplitude TMS-artifacts between -2 to 8 ms were removed from each trial and then the

remaining data segments were concatenated. Then, ICA (round 1) was applied using pop_runica as implemented in EEGLAB, used with the FASTICA algorithm (*56*). To remove TMS decay artifacts, the three largest components explaining the variance between -150 to 150 ms were removed and other components were forward-projected. After the decay artifact was removed in this way, copies of these datasets were kept. Then, a 4th order Butterworth bandpass filter (0.5-45 Hz) and a 50 Hz notch filter (with a stopband of 45-55 Hz) were applied. A second round of ICA was applied to determine remaining TMS, ocular, muscle and cardiac artifacts. Afterwards, these ICA weights were applied on the copied dataset after the first round of ICA (unfiltered). After artifactual components were removed and the data was forward-projected, we further removed 15 ms post-stimulus window since TMS-evoked artifacts were still present in this time window. We then applied a cubic interpolation (for -2 to 15ms window) before applying the same filtering procedure (as described above) to the data. This way we ensured that the TMS artifacts did not smear into the post-stimulus window during the filtering process. Then, data was re-referenced offline to the average of the right and left mastoid signals and down-sampled to 500 Hz (**Fig. 7**).

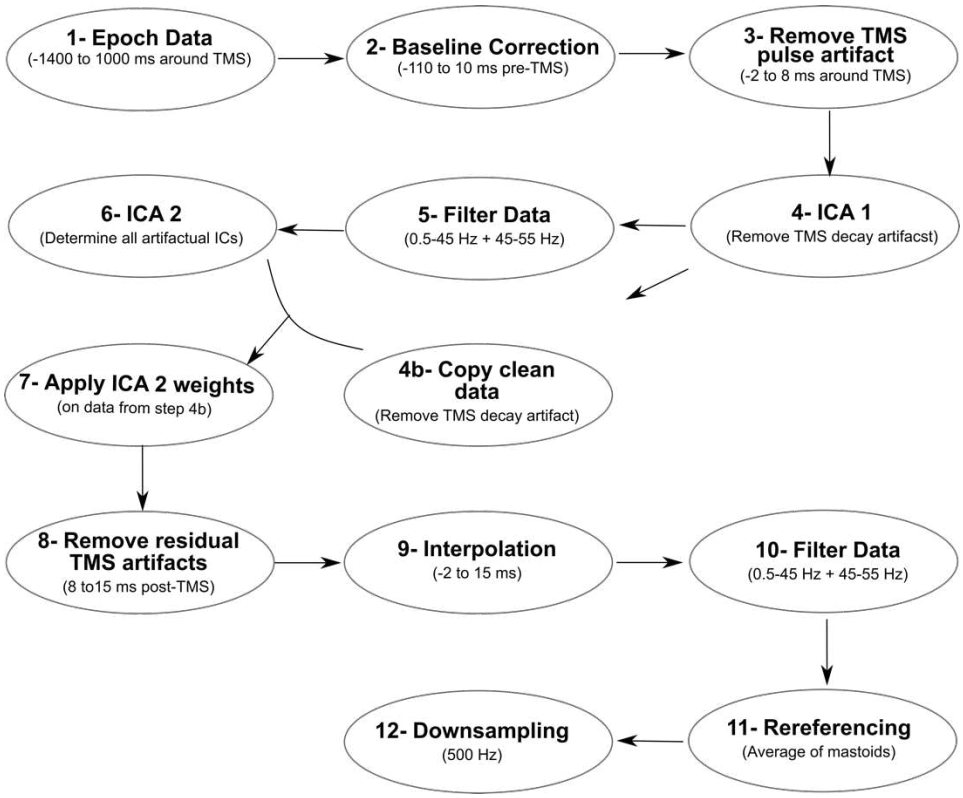

Figure 7. Preprocessing steps of EEG data for cleaning artifacts in the post-TMS window. These steps were followed before calculating TMS-evoked potentials (TEPs).

In further analyses of the TMS-EEG data, we only included trials in which TMS stimulation triggered a motor-evoked potential higher than 50 µV, which yielded on average 412 trials per subject. For the sham TMS condition, we only included trials, in which no evoked motor activity was observed (405 trials on average).

To assess cortical excitability in motor areas, we focused on early components of TMS-evoked potentials (TEPs) in the first 60 ms following the stimulation, since this time window specifically involves the activation of local neuronal populations in the motor cortex (*32*). Since the first 15 ms were interpolated, we evaluated TEPs between 15-60 ms in the post-TMS window in a cluster of electrodes over the right primary motor cortex (C4, CP4, C6, CP6). These electrodes were selected a priori since they were closest to the hotspot of the TMS stimulation.

Cardiac artifact during systole and diastole was estimated during TMS and sham conditions (see (*11*) for details on the pulse artifact cleaning of the evoked potentials) and subtracted from TMS-evoked potentials during systole and diastole individually.

<u>Heartbeat-Evoked Potentials</u>

In this analysis, we first analyzed the trials in which TMS stimulation was at least 400 ms after the previous R-peak (i.e., during diastole) to keep the heartbeat-evoked potential window free of TMS-related activity following previous studies (*11*, *13*). This allowed us to examine the relationship of HEPs (in response to heartbeats during systole) with MEPs (in response to TMS stimulation during diastole) within the same cardiac cycle. In this study, we also tested whether MEP amplitudes during the first 400 ms of the cardiac cycle are influenced by HEP activity from the previous cardiac cycle.

To clean TMS artifacts in the prestimulus window and keep data processing close to our previous work (*11*, *13*), some preprocessing steps were altered compared to the steps described above for the post-stimulation analyses: After the second round of ICA, we first calculated each distance between the prestimulus R peaks and TMS events. Then, we shuffled these distances and inserted “mock events” by subtracting them from the latency of TMS

stimulations in the dataset. Next, we repeated this shuffling process ten times. Finally, we segmented data between -100 to 400 ms around these mock events. By using an average of these segments, we derived an estimate of the TMS artifact in the time window of the heartbeat-evoked responses per subject.

We then subtracted this estimation from each heartbeat-evoked potential to remove any potential TMS artifacts. Finally, a baseline removal was performed, using the time window from -100 to 0 ms (relative to the R-peak).

Source Analyses

The neural sources of the TMS- and heartbeat-evoked potentials were reconstructed with the Brainstorm toolbox (*57*) using individually measured electrode positions with a TMS neuro-navigation system (Localite GmbH, Bonn, Germany). For every subject, the individual structural T1-weighted MRI images were segmented using Freesurfer (http://surfer.nmr.mgh.harvard.edu/). A 3-shell boundary element model (BEM) was constructed to calculate the lead field matrix with OpenMEEG (*58*, *59*). The lead field matrices were inverted using eLORETA individually for each contrast (e.g., TEP difference between systole and diastole) and participant. Individual source data were then projected to the ICBM152 template (*60*) and their absolute values were used in group averages.

Motor Pinch Task

After the TMS sessions, participants performed a pinch motor task. At the beginning of the task, their maximal pinch strength, i.e., maximal voluntary contraction (MVC), was calculated using SAEHAN® Hydraulic Hand Dynamometer Model SH5005 (SAEHAN Corporation, Korea). Participants were asked to squeeze the dynamometer with their left thumb pad against the lateral aspect of the middle phalanx of the left index finger as hard as possible while keeping their elbow in the 90° position. After calculating MVC, participants were asked to apply 30% of this contraction value (corresponding to 3.14 ± 0.88 pounds) when a green circle in the middle of the monitor returned to red. During the presentation of the red circle, which lasted for three seconds, they were asked to keep the contraction. When the circle became green again, they relaxed their hand for three seconds. In this order, subjects performed

632 contractions for thirty trials. The trials were categorized into systole and diastole according
633 to the movement onset of the subject after the visual cue (red circle).
634
635 EMG Envelope
636 To estimate muscle activity during the pinch task, EMG data were analyzed. First, the signal
637 was cleaned from movement-related artifacts and noise with the application of a 4^{th} order
638 Butterworth bandpass filter (10-500 Hz) and a 50 Hz notch filter (with a stopband of 45-55
639 Hz). Afterwards, the envelope of EMG was calculated by first taking the absolute value of the
640 signal ("full-wave rectification") and then applying a low pass filter (2^{nd} order Butterworth, 3
641 Hz) (*61*). The resulting EMG linear envelope was normalized by dividing it by the peak muscle
642 activation value during each trial. This was followed by a baseline correction using the -110
643 to -10ms pre-movement EMG signal. Finally, an average of the envelope was calculated when
644 pinch onset coincided with the systolic and diastolic phases of the cardiac cycle per subject.
645
646 Desynchronization of Sensorimotor Oscillations during the Motor Task
647 To investigate the central sensorimotor oscillations following pinch onset during systole and
648 diastole, we also analyzed EEG signals. For this purpose, we first filtered the data with a 4^{th}
649 order Butterworth bandpass (0.5-45 Hz) and a 50 Hz notch filter (with a stopband of 45-55
650 Hz). After cleaning muscular, cardiac, and ocular artifacts through ICA and re-referencing data
651 to the average of both mastoid electrodes, data were segmented between -1000 to 4000ms
652 around the pinch onset. We then performed a Morlet wavelet analysis to investigate
653 sensorimotor alpha and beta activity locked to pinch onset. This analysis was performed on
654 every trial for frequencies from 5 to 40 Hz with the number of cycles increasing linearly from
655 4 to 10. Thus, a wavelet at 10 Hz was 4.9 cycles long, had a temporal resolution of 0.10 s and
656 a spectral resolution of 4.85 Hz. We then calculated the average time-frequency activity for
657 each cardiac phase per subject.
658
659 Statistics
660 We statistically tested the two-condition comparisons of TEPs, HEPs, EMG linear envelope
661 and sensorimotor oscillations using cluster-based permutation *t*-tests as implemented in the
662 FieldTrip toolbox (*62*). To define clusters, the default threshold value ($p<0.05$, two-tailed) was
663 used. To test cluster-level statistics, condition labels were randomly shuffled 1,000 times to

estimate the distribution of maximum cluster-level statistics obtained by chance. We report the temporal windows and spatial regions that we tested for each individual analysis below.

Statistical analysis of TEP activity during systole and diastole were conducted at electrodes C4, CP4, C6, and CP6 between 15 and 60 ms. Pre- and post-TMS changes in heart rate for stimulation during systole and diastole were evaluated using within-subject ANOVAs (ezANOVA function in R (*63*, *64*)), in which heart rate was the dependent variable and time (pre-TMS, TMS, post-TMS) as well as cardiac phase (systole, diastole) were independent variables. For statistical testing of HEP activity relating to motor excitability, we first sorted single trials according to their MEP amplitudes and split them into three equal bins for each participant. For the weakest and strongest MEP bins, we then contrasted prestimulus HEP amplitudes between 296 and 400 ms in a cluster of electrodes (FC2, Cz, C4, CP1, CP2, Pz, P4, C1, C2, CPz, CP4, P1, P2), where we previously observed significant modulations of HEP preceding somatosensory processes (*11*, *13*). In the cluster analysis of both TEPs and HEPs, clusters were formed in the spatiotemporal domain using the a priori defined set of electrodes and temporal windows.

During the motor task, the statistical analysis focused on the first second of the muscle contraction following the pinch onset, as cardiac effect are expected to be transient and may last for one cardiac cycle only. Therefore, statistical analysis of the EMG envelope during systole and diastole were conducted in the time window of 0-1000 ms. During the same time window, sensorimotor oscillations were compared in the range of 8-30 Hz over a set of electrodes over sensorimotor regions (C4, CP4, C6, CP6) using cluster statistics, in order to account for multiple comparisons in the temporal, spatial and frequency domain.

Repeated measures correlation coefficient was calculated to test the changes in the heart rate across the motor excitability levels by using ‘rmcorr’ function (*65*) in R (v 1.3.1093).

Linear-Mixed-Effects Model

To test the relationship between MEP amplitudes and the distance from the previous heartbeat, linear-mixed-effects models were fitted on the single-trial level. First, we hierarchically compared a null model, which assumes no relationship (MEP~ (1 | subject) to a

model which assumes a linear relationship between MEP amplitudes and the distance (MEP ~ distance + (1 | subject)). Then, we compared this linear model to a second-degree polynomial model (MEP)~ distance + distance^2+ (1 | subject). In these models, we used the natural logarithmic transformation of MEP amplitudes.

Data and code availability

The experimental code and analysis scripts are available at https://github.com/Esra-Al/Cardiac_Motor_TMS_EEG. The datasets generated during the current study are available from the corresponding author on reasonable request. Due to a lack of explicit consent on the part of the participants to data sharing, structural MRI and EEG data cannot be shared publicly. Such data can only be shared if data privacy can be guaranteed according to the rules of the European General Data Protection Regulation.

Author contributions

E.A., T.S., M.E., A.V., and V.N. designed the experiment, E.A. acquired the data. E.A., T.S., and V.N. analyzed the data. E.A., T.S, A.V., and V.N. wrote the paper.

Competing Interests

The authors declare that they have no competing financial interests.

References

1. M. Allen, D. Frank, D. Samuel Schwarzkopf, F. Fardo, J. S. Winston, T. U. Hauser, G. Rees, Unexpected arousal modulates the influence of sensory noise on confidence. *Elife*. **5** (2016), doi:10.7554/ELIFE.18103.
2. H. D. Critchley, S. N. Garfinkel, The influence of physiological signals on cognition. *Curr. Opin. Behav. Sci.* **19**, 13–18 (2018).
3. D. Azzalini, I. Rebollo, C. Tallon-Baudry, Visceral Signals Shape Brain Dynamics and Cognition. *Trends Cogn. Sci.* **23**, 488–509 (2019).
4. O. Perl, A. Ravia, M. Rubinson, A. Eisen, T. Soroka, N. Mor, L. Secundo, N. Sobel, Human non-olfactory cognition phase-locked with inhalation. *Nat. Hum. Behav. 2019 35*. **3**, 501–512 (2019).
5. H.-D. Park, C. Barnoud, H. Trang, O. A. Kannape, K. Schaller, O. Blanke, Breathing is

coupled with voluntary action and the cortical readiness potential. *Nat. Commun. 2020 111*. **11**, 1–8 (2020).

6. M. Grund, E. Al, M. Pabst, A. Dabbagh, T. Stephani, T. Nierhaus, M. Gaebler, A. Villringer, *J. Neurosci.*, in press, doi:10.1523/JNEUROSCI.0592-21.2021.

7. C. A. Sandman, T. R. McCanne, D. N. Kaiser, B. Diamond, Heart rate and cardiac phase influences on visual perception. *J. Comp. Physiol. Psychol.* **91**, 189–202 (1977).

8. S. A. Saxon, Detection of near threshold signals during four phases of cardiac cycle. *Ala. J. Med. Sci.* **7**, 427–30 (1970).

9. M. Van Elk, B. Lenggenhager, L. Heydrich, O. Blanke, Suppression of the auditory N1-component for heartbeat-related sounds reflects interoceptive predictive coding. *Biol. Psychol.* **99**, 172–182 (2014).

10. M. Wilkinson, D. McIntyre, L. Edwards, Electrocutaneous pain thresholds are higher during systole than diastole. *Biol. Psychol.* **94**, 71–73 (2013).

11. E. Al, F. Iliopoulos, N. Forschack, T. Nierhaus, M. Grund, P. Motyka, M. Gaebler, V. V. Nikulin, A. Villringer, Heart-brain interactions shape somatosensory perception and evoked potentials. *Proc. Natl. Acad. Sci. U. S. A.* **117**, 10575–10584 (2020).

12. P. Motyka, M. Grund, N. Forschack, E. Al, A. Villringer, M. Gaebler, Interactions between cardiac activity and conscious somatosensory perception. *Psychophysiology*, e13424 (2019).

13. E. Al, F. Iliopoulos, V. V. Nikulin, A. Villringer, Heartbeat and somatosensory perception. *Neuroimage*. **238**, 118247 (2021).

14. S. Duschek, N. S. Werner, G. A. R. del Paso, The behavioral impact of baroreflex function: A review. *Psychophysiology*. **50**, 1183–1193 (2013).

15. L. Edwards, C. Ring, D. McIntyre, D. Carroll, U. Martin, Psychomotor speed in hypertension: Effects of reaction time components, stimulus modality, and phase of the cardiac cycle. *Psychophysiology*. **44**, 459–468 (2007).

16. M. J. Saari, B. A. Pappas, Cardiac Cycle Phase and Movement and Reaction Times. *Percept. Mot. Skills*. **42**, 767–770 (1976).

17. A. Galvez-Pol, R. McConnell, J. M. Kilner, Active sampling in visual search is coupled to the cardiac cycle. *Cognition*. **196** (2020), doi:10.1016/j.cognition.2019.104149.

18. S. Ohl, C. Wohltat, R. Kliegl, O. Pollatos, R. Engbert, Microsaccades are coupled to heartbeat. *J. Neurosci.* **36**, 1237–1241 (2016).

19. S. Kunzendorf, F. Klotzsche, M. Akbal, A. Villringer, S. Ohl, M. Gaebler, Active information sampling varies across the cardiac cycle. *Psychophysiology*. **56**, 1–16 (2019).
20. E. R. Palser, J. Glass, A. Fotopoulou, J. M. Kilner, Relationship between cardiac cycle and the timing of actions during action execution and observation. *Cognition*. **217** (2021), doi:10.1016/J.COGNITION.2021.104907.
21. A. M. Herman, M. Tsakiris, Feeling in Control: The Role of Cardiac Timing in the Sense of Agency. *Affect. Sci. 2020 13*. **1**, 155–171 (2020).
22. N. Konttinen, T. Mets, H. Lyytinen, M. Paananen, Timing of triggering in relation to the cardiac cycle in nonelite rifle shooters. *Res. Q. Exerc. Sport*. **74**, 395–400 (2003).
23. H.-D. Park, S. Correia, A. Ducorps, C. Tallon-Baudry, Spontaneous fluctuations in neural responses to heartbeats predict visual detection. *Nat. Neurosci.* **17**, 612–618 (2014).
24. E. Bianchini, M. Mancuso, A. Zampogna, A. Guerra, A. Suppa, Cardiac cycle does not affect motor evoked potential variability: A real-time EKG-EMG study. *Brain Stimul. Basic, Transl. Clin. Res. Neuromodulation*. **14**, 170–172 (2021).
25. P. H. Ellaway, N. J. Davey, D. W. Maskill, S. R. Rawlinson, H. S. Lewis, N. P. Anissimova, Variability in the amplitude of skeletal muscle responses to magnetic stimulation of the motor cortex in man. *Electroencephalogr. Clin. Neurophysiol. Mot. Control*. **109**, 104–113 (1998).
26. N. Otsuru, S. Miyaguchi, S. Kojima, K. Yamashiro, D. Sato, H. Yokota, K. Saito, Y. Inukai, H. Onishi, Timing of Modulation of Corticospinal Excitability by Heartbeat Differs with Interoceptive Accuracy. *Neuroscience*. **433**, 156–162 (2020).
27. M. M. Filippi, M. Oliveri, F. Vernieri, P. Pasqualetti, P. M. Rossini, Are autonomic signals influencing cortico-spinal motor excitability?: A study with transcranial magnetic stimulation. *Brain Res.* **881**, 159–164 (2000).
28. H. Mäki, R. J. Ilmoniemi, The relationship between peripheral and early cortical activation induced by transcranial magnetic stimulation. *Neurosci. Lett.* **478**, 24–28 (2010).
29. N. C. Rogasch, Z. J. Daskalakis, P. B. Fitzgerald, Mechanisms underlying long-interval cortical inhibition in the human motor cortex: A TMS-EEG study. *J. Neurophysiol.* **109**, 89–98 (2013).

30. X. Zhong, C. H. Meyer, D. J. Schlesinger, J. P. Sheehan, F. H. Epstein, J. M. Larner, S. H. Benedict, P. W. Read, K. Sheng, J. Cai, Tracking brain motion during the cardiac cycle using spiral cine-DENSE MRI. *Med. Phys.* **36**, 3413–3419 (2009).
31. H. Morita, J. Baumgarten, N. Petersen, L. O. D. Christensen, J. Nielsen, Recruitment of extensor-carpi-radialis motor units by transcranial magnetic stimulation and radial-nerve stimulation in human subjects. *Exp. brain Res.* **128**, 557–562 (1999).
32. S. Harquel, T. Bacle, L. Beynel, C. Marendaz, A. Chauvin, O. David, Mapping dynamical properties of cortical microcircuits using robotized TMS and EEG: Towards functional cytoarchitectonics. *Neuroimage*. **135**, 115–124 (2016).
33. M. E. Wagshul, P. K. Eide, J. R. Madsen, The pulsating brain: A review of experimental and clinical studies of intracranial pulsatility. *Fluids Barriers CNS*. **8** (2011), pp. 1–23.
34. J. H. Lawrence, C. J. De Luca, Myoelectric signal versus force relationship in different human muscles. *J. Appl. Physiol.* **54**, 1653–1659 (1983).
35. G. Pfurtscheller, A. Stancak, C. Neuper, C. Neuper, Event-related synchronization (ERS) in the alpha band -an electrophysiological correlate of cortical idling: A review. *Int. J. Psychophysiol.* **24**, 39–46 (1996).
36. G. Pfurtscheller, F. H. Lopes da Silva, Event-related EEG/MEG synchronization and desynchronization: basic principles. *Clin. Neurophysiol.* **110**, 1842–1857 (1999).
37. M. Allen, A. Levy, T. Parr, K. J. Friston, In the Body's Eye: The Computational Anatomy of Interoceptive Inference. *bioRxiv*, 603928 (2019).
38. R. J. Milne, A. M. Aniss, N. E. Kay, S. C. Gandevia, Reduction in perceived intensity of cutaneous stimuli during movement: a quantitative study. *Exp. brain Res.* **70**, 569–576 (1988).
39. A. Starr, L. G. Cohen, "Gating" of somatosensory evoked potentials begins before the onset of voluntary movement in man. *Brain Res.* **348**, 183–186 (1985).
40. K. Seki, E. E. Fetz, Gating of Sensory Input at Spinal and Cortical Levels during Preparation and Execution of Voluntary Movement. *J. Neurosci.* **32**, 890 (2012).
41. C. L. Rae, A. Ahmad, D. E. O. Larsson, M. Silva, C. D. G. van Praag, S. N. Garfinkel, H. D. Critchley, Impact of cardiac interoception cues and confidence on voluntary decisions to make or withhold action in an intentional inhibition task. *Sci. Rep.* **10** (2020), doi:10.1038/S41598-020-60405-8.
42. L. Edwards, K. Inui, C. Ring, X. Wang, R. Kakigi, Pain-related evoked potentials are

824 modulated across the cardiac cycle. *PAIN®*. **137**, 488–494 (2008).
825 43. H.-D. Park, O. Blanke, Heartbeat-evoked cortical responses: Underlying mechanisms,
826 functional roles, and methodological considerations. *Neuroimage*. **197**, 502–511
827 (2019).
828 44. D. M. Blumberger, F. Vila-Rodriguez, K. E. Thorpe, K. Feffer, Y. Noda, P. Giacobbe, Y.
829 Knyahnytska, S. H. Kennedy, R. W. Lam, Z. J. Daskalakis, J. Downar, Effectiveness of
830 theta burst versus high-frequency repetitive transcranial magnetic stimulation in
831 patients with depression (THREE-D): a randomised non-inferiority trial. *Lancet*. **391**,
832 1683–1692 (2018).
833 45. H. Johansen-Berg, M. F. Rushworth, M. D. Bogdanovic, U. Kischka, S. Wimalaratna, P.
834 M. Matthews, The role of ipsilateral premotor cortex in hand movement after stroke.
835 *Proc. Natl. Acad. Sci. U. S. A.* **99**, 14518–14523 (2002).
836 46. K. Udupa, T. N. Sathyaprabha, J. Thirthalli, K. R. Kishore, T. R. Raju, B. N. Gangadhar,
837 Modulation of cardiac autonomic functions in patients with major depression treated
838 with repetitive transcranial magnetic stimulation. *J. Affect. Disord.* **104**, 231–236
839 (2007).
840 47. T. A. Iseger, F. Padberg, J. L. Kenemans, R. Gevirtz, M. Arns, Neuro-Cardiac-Guided
841 TMS (NCG-TMS): Probing DLPFC-sgACC-vagus nerve connectivity using heart rate –
842 First results. *Brain Stimul.* **10**, 1006–1008 (2017).
843 48. M. Kaur, J. A. Michael, K. E. Hoy, B. M. Fitzgibbon, M. S. Ross, T. A. Iseger, M. Arns, A.-
844 R. Hudaib, P. B. Fitzgerald, Investigating high- and low-frequency neuro-cardiac-
845 guided TMS for probing the frontal vagal pathway. *Brain Stimul. Basic, Transl. Clin.*
846 *Res. Neuromodulation*. **13**, 931–938 (2020).
847 49. C. D. B. Luft, J. Bhattacharya, Aroused with heart: Modulation of heartbeat evoked
848 potential by arousal induction and its oscillatory correlates. *Sci. Rep.* **5**, 1–11 (2015).
849 50. O. Löfberg, P. Julkunen, A. Pääkkönen, J. Karhu, The auditory-evoked arousal
850 modulates motor cortex excitability. *Neuroscience*. **274**, 403–408 (2014).
851 51. A. Azarbarzin, M. Ostrowski, P. Hanly, M. Younes, Relationship between arousal
852 intensity and heart rate response to arousal. *Sleep*. **37**, 645–653 (2014).
853 52. T. Stephani, G. Waterstraat, S. Haufe, G. Curio, A. Villringer, V. V. Nikulin, Temporal
854 Signatures of Criticality in Human Cortical Excitability as Probed by Early
855 Somatosensory Responses. *J. Neurosci.* **40**, 6572–6583 (2020).

53. R. C. Oldfield, The assessment and analysis of handedness: The Edinburgh inventory. *Neuropsychologia*. **9**, 97–113 (1971).
54. V. Nikouline, J. Ruohonen, R. J. Ilmoniemi, The role of the coil click in TMS assessed with simultaneous EEG. *Clin. Neurophysiol.* **110**, 1325–1328 (1999).
55. C. R. Vázquez-Seisdedos, J. E. Neto, E. J. Marañón Reyes, A. Klautau, R. C. Limão de Oliveira, New approach for T-wave end detection on electrocardiogram: performance in noisy conditions. *Biomed. Eng. Online*. **10**, 77 (2011).
56. A. Hyvärinen, Fast and robust fixed-point algorithms for independent component analysis. *IEEE Trans. Neural Networks*. **10**, 626–634 (1999).
57. F. Tadel, S. Baillet, J. C. Mosher, D. Pantazis, R. M. Leahy, Brainstorm: A user-friendly application for MEG/EEG analysis. *Comput. Intell. Neurosci.* **2011** (2011), doi:10.1155/2011/879716.
58. J. Kybic, M. Clerc, T. Abboud, O. Faugeras, R. Keriven, T. Papadopoulo, A common formalism for the Integral formulations of the forward EEG problem. *IEEE Trans. Med. Imaging*. **24**, 12–28 (2005).
59. A. Gramfort, T. Papadopoulo, E. Olivi, M. Clerc, OpenMEEG: opensource software for quasistatic bioelectromagnetics. *Biomed. Eng. Online*. **9**, 45 (2010).
60. V. Fonov, A. Evans, R. McKinstry, C. Almli, D. Collins, Unbiased nonlinear average age-appropriate brain templates from birth to adulthood. *Neuroimage*. **47**, S102 (2009).
61. D. A. Winter, Biomechanics and Motor Control of Human Movement: Fourth Edition. *Biomech. Mot. Control Hum. Mov. Fourth Ed.*, 1–370 (2009).
62. R. Oostenveld, P. Fries, E. Maris, J.-M. Schoffelen, FieldTrip: Open Source Software for Advanced Analysis of MEG, EEG, and Invasive Electrophysiological Data. *Comput. Intell. Neurosci.* **2011**, 1–9 (2011).
63. M. Lawrence, ez: Easy Analysis and Visualization of Factorial Experiments. (2016), (available at https://cran.r-project.org/package=ez).
64. R Development Core Team, R: A Language and Environment for Statistical Computing. (2021).
65. J. Bakdash, L. Marusich, rmcorr: Repeated Measures Correlation (2021), (available at https://cran.r-project.org/package=rmcorr).
66. R. D. Morey, Confidence Intervals from Normalized Data: A correction to Cousineau (2005). *Tutor. Quant. Methods Psychol.* **4**, 61–64 (2008).

Supplementary Files

This is a list of supplementary files associated with this preprint. Click to download.

- SupplementaryFiguresTMSEEG.pdf